Vol. 47: 171–186, 2011
doi: 10.3354/cr00990

CLIMATE RESEARCH
Clim Res

Published online June 29

# Performance of Regional Climate Model RegCM3 over Thailand

**Mega Octaviani[1,2], Kasemsan Manomaiphiboon[1,2,*]**

[1]The Joint Graduate School of Energy and Environment (JGSEE), King Mongkut's University of Technology Thonburi (KMUTT), Bangkok 10140, Thailand

[2]Center for Energy Technology and Environment, Ministry of Education, Bangkok 10300, Thailand

ABSTRACT: This study assesses the performance of the regional climate model RegCM3 and its sensitivity to selected physical parameterizations and 1-way double nesting over Thailand. A total of 16 simulation experiments were conducted using different combinations of convective and ocean flux parameterization schemes on a 60 km resolution (D1) and a nested 20 km resolution (D2) domain. The simulated results were compared with the Thai Meteorological Department (TMD) data for (near-surface) temperature and precipitation, and ERA40 reanalysis data for upper-level synoptic winds. In both the D1 and D2 experiments, considerable systematic underestimation of temperature was found for the upper sub-regions (Central-East, Northeast, and North) of Thailand with the maximum cold bias of 6.0°C. Seasonal discrepancies (between dry and wet seasons) in precipitation, as observed in these sub-regions, were well captured. Over the lower sub-region (South), cold biases were smaller than in the upper sub-regions, and the relatively high rates of precipitation normally observed in the dry season were reproduced by the model. The main features of seasonal synoptic winds were fairly simulated with better performance seen in the dry season. For the convective parameterization schemes, MIT-Emanuel performed best on temperature, followed by Anthes-Kuo. However, in the wet season, the former scheme produced large wet biases, particularly for the upper sub-regions. Grell-Arakawa-Schubert yielded smaller cold biases than Grell-Fritsch-Chappell, but their relative performances on precipitation were not conclusive. For ocean flux parameterization, the BATS scheme, in comparison with the Zeng scheme, provided better predictions for temperature and yielded more precipitation. The nested modeling enhanced the spatial details of model outputs but did not necessarily improve the overall performance in a particular sub-region. A gridded observation dataset from the University of Delaware (UDEL) was used to qualitatively examine the model performance on temperature and precipitation, and reasonable agreement was found for both TMD and UDEL datasets. An additional simulation test was conducted to examine the effect of a land cover modification (here, from 'irrigated crop' to 'crop/mixed farming') as a potential technique to alleviate the problem of temperature underestimation. It was found that using the modified land cover helped reduce the degree of bias by 2.2 to 3.3°C in the upper sub-regions during the dry season.

KEY WORDS: Model performance · Sensitivity · Convective parameterization · Ocean flux parameterization · Nesting · Land cover · Thailand



## 1. INTRODUCTION

Regional climate models (RCMs) are typically used to downscale meteorological or climatic information at a coarse resolution (e.g. reanalysis data and outputs generated from a global climate model or GCM) to a finer spatial resolution. A GCM simulates features at the global scale with a resolution of a few hundred km. Although GCMs produce key synoptic-scale atmospheric circulations, some small-scale or subgrid pro-

*Corresponding author. Email: kasemsan_m@jgsee.kmutt.ac.th

cesses (especially those associated with land surface), are omitted or not sufficiently accounted for, which could be remedied by use of a RCM. Several RCMs have been developed, advanced, made available to, and are used by scientific communities. They have become an essential tool for the assessment of climate and its variability at a regional scale, with a typical resolution of tens of km (Giorgi et al. 2001, Christensen et al. 2007).

Thailand is a tropical country located in the middle of continental Southeast Asia (i.e. the Indochinese Peninsula), and has diverse topography. It is greatly influenced by the 2 prevailing monsoons, southwest and northeast (TMD 2008). The southwest monsoon starts in mid-May and ends in mid-October, carrying warm moist air from the Indian Ocean and causing the rainy or wet season for most of the country. The north–south movement of the inter-tropical convergence zone (ITCZ) also increases the intensity of rainfall over the sub-region. The northeast monsoon usually starts in mid-October and ends in mid-February, carrying cold, dry, continental air masses from the mid-latitudes (i.e. China and the South China sea) and causing the winter and dry season. However, as the air masses travel further south through the Gulf of Thailand, they gain moisture and bring abundant rains to the southern part of Thailand. During a transitional period between the 2 monsoons, tropical cyclones sometimes develop in the Bay of Bengal, South China Sea, and Pacific Ocean, producing heavy rains in many coastal areas. Moreover, the climate of the sub-region is modulated by different topography in different sub-sub-regions — valleys and mountains in the North, a broad plateau in the Northeast, a large alluvial plain with sporadic hills in the Central and Eastern areas, and a mix of coastal plains and mountains in the South. Accordingly, regional climate modeling, specifically adapted for Thailand, is needed.

The RCM chosen for the present study is RegCM3, which is a community-based open-source freely-distributed model. RegCM3 is the latest generation of the National Center for Atmospheric Research (NCAR) RCM developed in the late 1980s (Elguindi et al. 2006, Pal et al. 2007). The model has undergone several improvements from the previous version RegCM2 (Giorgi et al. 1993a,b), which are mainly (1) the representation of radiative transfer and large-scale precipitation processes, (2) new parameterizations for ocean flux and cumulus convection schemes, and (3) the inclusion of 1-way double nesting and subgrid-scale topography. The model continues to be developed and maintained under support from the Abdus Salam International Center for Theoretical Physics (ICTP), Italy. The model offers numerous physics and modeling options and provides interfaces for various input datasets. It has been used for regional climate studies in many areas (Pal et al. 2007 and references therein). For Southeast Asia, the use of RegCM3 has been limited but the model is gaining interest from regional scientific communities (Francisco et al. 2006, Phan et al. 2009). For Thailand, to the authors' knowledge, only a few regional climate modeling studies have been conducted, e.g. Southeast Asia START Regional Center (2009), and no RegCM3 applications have been found. In applying a RCM for a particular purpose, it is critical to first investigate the RCM's prediction capability in order to better understand its strengths and weaknesses and potential biases arising from modeling; this formed the motivational basis of this study. Such information is also useful to guide users on customization of the model in the future and model developers on existing model limitations and directions for future improvement.

It is commonly known that an adequate representation of physical parameterization schemes in a RCM is essential and greatly influences the characteristics or quality of simulated results. Many studies have examined the sensitivity of a RegCM-family model (e.g. RegCM2 and RegCM3) to different modeling options or configurations, e.g. Seth & Giorgi (1998) on domain size and initial soil moisture, Gao et al. (2006) on modeling resolutions and topography, Francisco et al. (2006) on driving lateral boundary conditions and ocean flux schemes, Martinez-Castro et al. (2006) on convective schemes at different domain resolutions and ocean flux schemes, and Im et al. (2008) on convective schemes in 2 nested domains. In the present study, we assessed the overall performance of RegCM3 over Thailand, and determined how sensitive simulated results could be to different choices of the 4 available convective parameterization schemes (CPSs), and the 2 available ocean flux parameterization schemes (OFSs), in order to understand the applicability of the model for Thailand. The convective and ocean flux parameterizations are considered here because each represents a physical process essential in atmospheric modeling and has multiple options offered in the model. It is also of interest to examine the capability of the 1-way double nesting to enhance the quality of simulated results. The meteorological variables considered are near-surface temperature (to be referred to as temperature) and precipitation, which are the 2 most essential climate variables. The evaluation was extended to examine the featured characteristics of upper-level synoptic winds prevailing during the 2 monsoonal periods in the sub-region. Doing so may help to understand the model's existing capabilities and suggest the strengths and weaknesses of the model for its future use for Thailand.

## 2. METHODOLOGY

### 2.1. Model description

RegCM3 is a hydrostatic and compressible model, and its dynamical core is based on that of the NCAR-Penn State University (PSU) Mesoscale Model version 5 (MM5) (Grell et al. 1994). The model uses the terrain-following sigma-pressure coordinate. In the version used for the present study, the model includes the radiation parameterization of the NCAR Community Climate Model version 3 (CCM3) (Kiehl et al. 1996), and the land-surface model of Biosphere-Atmosphere Transfer Scheme (BATS) version 1e (Dickinson et al. 1993). The planetary boundary layer (PBL) is parameterized in accordance with Holtslag et al. (1990). The resolvable-scale precipitation is computed by the Subgrid Explicit Moisture scheme (SUBEX) (Pal et al. 2000). Two schemes representing ocean–atmosphere exchanges of surface fluxes of heat, moisture, and momentum are the BATS scheme (Dickinson et al. 1993) and the scheme proposed by Zeng et al. (1998) (an ocean flux parameterization scheme, henceforth the 'Zeng scheme'), both of which use a bulk aerodynamic approach for the computation of surface fluxes. The former scheme assumes a constant roughness length of 0.0024 m. The latter scheme allows roughness length to vary with friction velocity and stability condition so that it tends to correct the tendency of other schemes to overestimate latent heat flux under either very weak or very strong wind conditions (Zeng et al. 1998).

There are 4 CPSs available in the model. The first is the Anthes-Kuo (AK) scheme (Anthes 1977). The AK scheme is based on a column-integrated moisture convergence closure and environmental instability, without any parameterization on updraft and downdraft. Whenever the column is conditionally unstable and the moisture convergence exceeds a critical value, a portion of this moisture convergence will form cloud and rainfall, and the rest will increase the moisture of the column. The second is the Grell scheme (Grell 1993). This scheme simulates clouds as an updraft and a downdraft that mix with the environment only at the cloud top and bottom. Convection is activated when a parcel lifted from the updraft originating levels (given by the level of maximum moist static energy) reaches saturation. Precipitation is calculated as the updraft condensation minus the downdraft evaporation. The Grell scheme can be further implemented using one of the following 2 closures: (1) the Arakawa and Schubert closure (Arakawa & Schubert 1974), and (2) the Fritsch and Chappell closure (Fritsch & Chappell 1980), to be referred to as Grell Arakawa Schubert (GAS) and Grell Fritsch Chappell (GFC), respectively. The GAS closure relates the amount of convection to the rate of destabilization of the environment, which means that convection tends to stabilize the environment as fast as large-scale processes tend to increase the total available buoyant energy (ABE). The GFC closure assumes that convection removes the ABE over a specified time scale and, thus, no dependencies on the large-scale processes. Both closures reach a statistical equilibrium between convection and the large-scale processes (Elguindi et al. 2006). The last scheme is the MIT-Emanuel (EMU) scheme (Emanuel 1991, Emanuel & Zivkovic-Rothman 1999), which is the most recent CPS included in RegCM3. The main difference from the other CPSs is that subcloud-scale updrafts and downdrafts are the primary elements used to represent moist convective transports, rather than the clouds themselves. Convection is activated when the level of neutral buoyancy is above the cloud base. Air is lifted between these 2 levels and part of the condensed moisture falls as rain, whereas the remaining moisture forms the cloud. Air from the environment is mixed into the cloud and forms a a spectrum of mixtures of differing mixing fractions which then ascend or descend according to their buoyancy. The scheme creates many mixing episodes and assumes that the mixed air detrains at levels where liquid water potential temperature equals that of its environment (Emanuel 1991).

### 2.2. Model configuration and experiment design

The RegCM3 model was run on 2 modeling domains chosen for simulations, Domain 1 (D1) and Domain 2 (D2), with 1-way double nesting. The former has a horizontal grid resolution of 60 km (considered coarse resolution) and covers the Indochinese Peninsula, part of Southern China, and part of South Asia (Fig. 1a). The latter is a nested domain and has a finer resolution of 20 km, covering Thailand, Laos, Cambodia, and most of Vietnam and Myanmar (Fig. 1b). Each domain has 100 × 100 grid cells and 18 sigma layers (full sigma values: 1.0, 0.99, 0.98, 0.96, 0.93, 0.89, 0.84, 0.78, 0.71, 0.63, 0.55, 0.47, 0.39, 0.31, 0.23, 0.16, 0.10, 0.05, and 0.0) with the top pressure at 100 hPa. Both domains use a Lambert conformal conic (LCC) projection and are centered at 13.5° N, 100.5° E. The initial and lateral boundary conditions for D1 were the European Centre for Medium-Range Weather Forecasts (ECMWF) 40 yr reanalysis data (ERA40) (Uppala et al. 2005). The data have a 2.5° resolution with 6 h intervals and 23 pressure levels with the top pressure at 1 hPa. The exponential relaxation method was employed, with a buffer zone of 12 grid points from lateral boundaries (Giorgi et al. 1993b). The boundary conditions were updated

every 6 h for both domains. Sea surface temperature (SST) data were taken from the weekly-average 1° resolution Optimum Interpolation SST (OISST) data of the National Ocean and Atmosphere Administration (NOAA) (Reynolds et al. 2002). Terrain elevation data were taken from the Global Topographic 30-arc-second data (GTOPO30) of the US Geological Survey (USGS 1996). The land use/land cover data were from the USGS Global Land Cover Characterization (GLCC) data, with BATS classification (Loveland et al. 2000).

A total of 16 sensitivity experiments were formed by combining the 4 CPSs (AK, GAS, GFC, and EMU) and the 2 OFSs (BATS and Zeng) (Table 1). The first 8

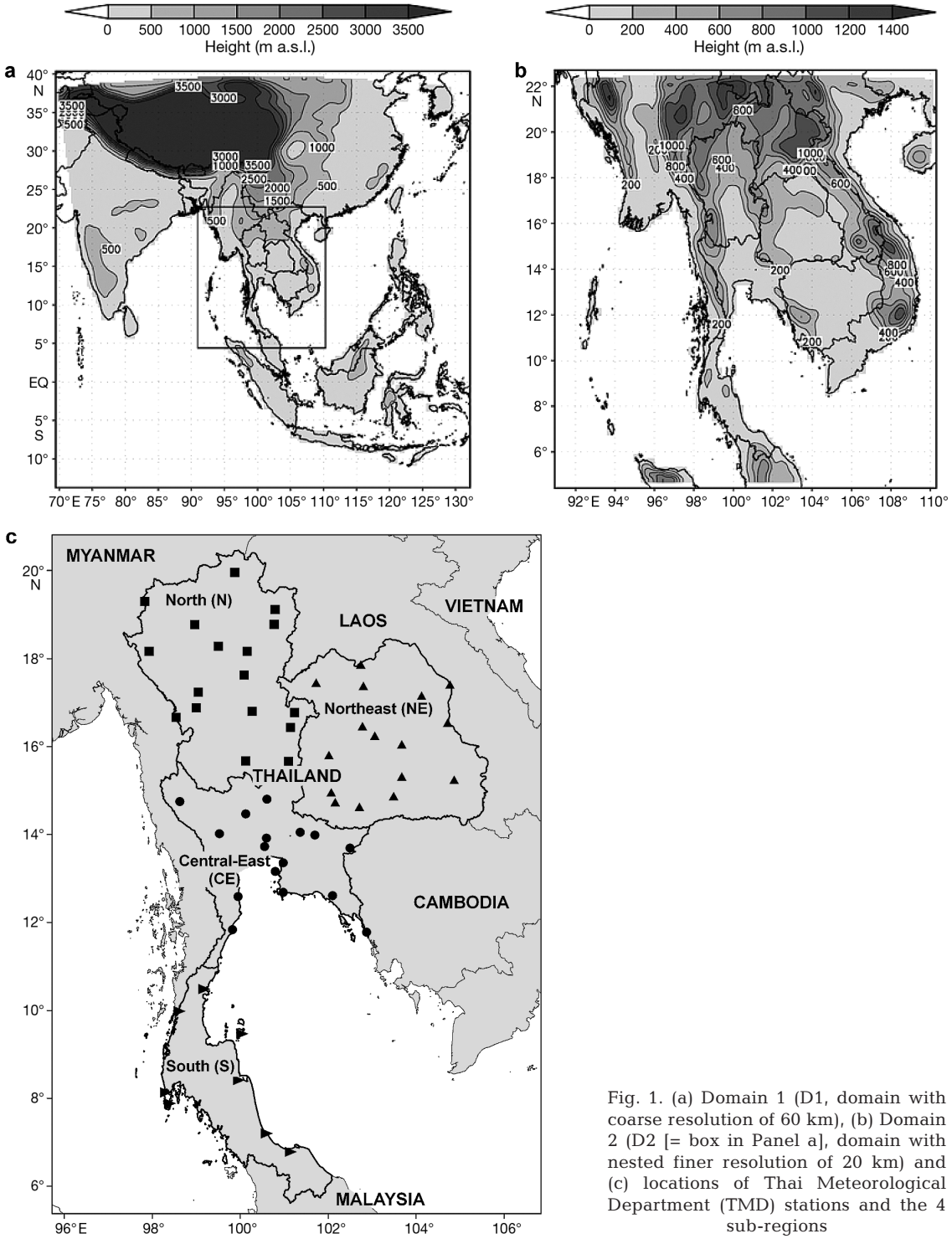


Fig. 1. (a) Domain 1 (D1, domain with coarse resolution of 60 km), (b) Domain 2 (D2 [= box in Panel a], domain with nested finer resolution of 20 km) and (c) locations of Thai Meteorological Department (TMD) stations and the 4 sub-regions

Table 1. Experiment design. CPS: convective parameterization schemes; OFS: ocean flux parameterization schemes; E1–E8: 8 experiments conducted on a coarse resolution domain (D1); E1N–E8N: 8 experiments conducted on a finer-resolution domain (D2); CPSs: Anthes-Kuo (AK), Grell-Arakawa-Schubert (GAS), Grell-Fritsch-Chappell (GFC), MIT-Emanuel (EMU); OFSs: Biosphere-Atmosphere Transfer Scheme (BATS), Zeng scheme (Zeng et al. 1998)

| No. | Experiment | CPS | OFS |
|---|---|---|---|
| **Resolution: 60 km** | | | |
| 1 | E1 | AK | Zeng |
| 2 | E2 | AK | BATS |
| 3 | E3 | GAS | Zeng |
| 4 | E4 | GAS | BATS |
| 5 | E5 | GFC | Zeng |
| 6 | E6 | GFC | BATS |
| 7 | E7 | EMU | Zeng |
| 8 | E8 | EMU | BATS |
| **Resolution: 20 km** | | | |
| 9 | E1N | AK | Zeng |
| 10 | E2N | AK | BATS |
| 11 | E3N | GAS | Zeng |
| 12 | E4N | GAS | BATS |
| 13 | E5N | GFC | Zeng |
| 14 | E6N | GFC | BATS |
| 15 | E7N | EMU | Zeng |
| 16 | E8N | EMU | BATS |

experiments (E1–E8) were conducted on the coarse domain (D1), while the rest (E1N–E8N), were conducted on the finer domain (D2) with nesting from the corresponding D1 experiments. The 2 simulation episodes are May 1997–February 1998, and May 1998–February 1999, with May used as spin-up time. These periods were selected for simulation because they fall within the temporal coverage (1997–1999) of the surface meteorological data provided by the Thai Meteorological Department (TMD), Ministry of Information and Communication Technology. Apart from the above experiments, an addition simulation test was carried out to examine the effects of land-cover modification on model results (as described in Section 3.4).

The observation data primarily used for the model evaluation was surface data from 58 stations selected from the TMD (Fig. 1c), and consisted of daily average air temperature (taken at 2 m above the ground), and daily accumulated precipitation. The total dataset was found to have missing values on average of ~13% per station. Synoptic winds at the pressure levels of 850 hPa and 200 hPa were investigated using the ERA40 reanalysis data. Only the D1 domain was used for synoptic wind evaluation due to its adequate spatial coverage for a synoptic scale. In addition, a gridded climatic dataset was used to qualitatively re-examine the overall model performance inferred from the TMD data. The gridded data were the publicly available monthly 0.5° resolution (over land only) temperature and precipitation taken from the global precipitation monthly grids for 1900–2008, University of Delaware v. 2.01 (Matsuura & Willmott 2009a,b) (hereafter, UDEL data). The UDEL data were developed from a sophisticated interpolation process on observations from global surface stations (over Thailand, 33 stations for temperature and 47 stations for precipitation). The UDEL data's temporal coverage fully covered the specified simulation periods. Besides the UDEL data, several other gridded climatic datasets are publicly available for use, e.g. Climate Research Unit (CRU) data, Tropical Rainfall Measuring Mission (TRMM) data, and Climate Prediction Center (CPC) GHCN-CAMS data. The choice of the UDEL data does not imply superiority over the others in terms of accuracy but is simply a supplementary dataset station-wise to the TMD data.

For the analysis, Thailand is divided into 4 sub-regions: Central-East (CE) which combines the Central and East sub-regions, Northeast (NE), North (N), and South (S) (see Fig. 1c) and 2 prevailing seasons (dry season: November–February, and wet season: June–September) (see Section 1). The typical climate of sub-regions CE, N and NE is generally continental, exhibiting the dry and wet seasons distinctly, whereas that of S is fairly maritime and not showing strong seasonality in precipitation.

The 2 main statistics used to evaluate the accuracy of the model predictions were the mean bias (MB) and the RMSE, which are calculated by

$$\mathrm{MB} = \frac{1}{N}\frac{1}{M}\sum_{j=1}^{N}\sum_{i=1}^{M}(P_{ij}-O_{ij}) \quad (1)$$

and

$$\mathrm{RMSE} = \sqrt{\frac{\sum_{j=1}^{N}\sum_{i=1}^{M}(P_{ij}-O_{ij})^2}{NM}} \quad (2)$$

where $O_{ij}$ is the observed daily ('daily average' for temperature and 'daily accumulated' for precipitation) value on day $i$ at station $j$ for a particular sub-region, $P_{ij}$ is the corresponding predicted daily value, $M$ is the total number of days in a particular season, and $N$ is the total number of stations used in a particular sub-region. Bilinear interpolation was used to interpolate the model output from neighboring grid cells to the location of a TMD station for point-wise (as opposed to gridded) comparison between an individual station and the model output. Box-and-whisker plots were used to examine the daily variability in both observed and simulated data, which is represented by the height of each box as an inter-quartile range (IQR = 3rd quartile – 1st quartile). In comparison with the UDEL data, simulated results were re-gridded to 0.5° resolution

according to the native grid structure of the data. For synoptic winds, the averaged wind vectors in each season are used in the analysis.

## 3. RESULTS AND DISCUSSION

### 3.1. Temperature

The model performance on temperature is summarized in Fig. 2 (with more details given in Tables S1 & S2 in the supplement at www.int-res.com/articles/suppl/c047p171_supp.pdf). For all D1 experiments, the model yielded underestimates (i.e. cold biases) for all 4 sub-regions, with MB and RMSE ranging from –6.0 to –0.1°C and 1.3 to 6.5°C, respectively, in the dry season. Improved results were seen in the wet season, with –4.8 to 0.2°C for MB and 1.2 to 5.2°C for RMSE. The upper sub-regions of Thailand (i.e. CE, NE, and N) had substantially large cold biases, particularly for N (>4°C in the dry season and >1°C in the wet season). In contrast, the lower sub-region of Thailand (i.e. S) had smaller cold biases (≤2°C in the dry season and <1°C in the wet season).

For the CPSs, the D1 experiments with GFC (i.e. E5 and E6) generally produced larger cold biases than those with GAS (E3 and E4), with E5 having the largest negative MB (largest RMSE), i.e. –6.0°C (6.5°C) in the dry season and –4.8°C (5.2°C) in the wet season. Using schemes AK (experiments E1 and E2) and EMU (E7 and E8) yielded smaller MB and RMSE magnitudes in most sub-regions. AK does not include a parameterization for the cooling effect of moist downdrafts and this may produce large errors in simulated precipitation (see Section 3.2). Using EMU gave the best results for

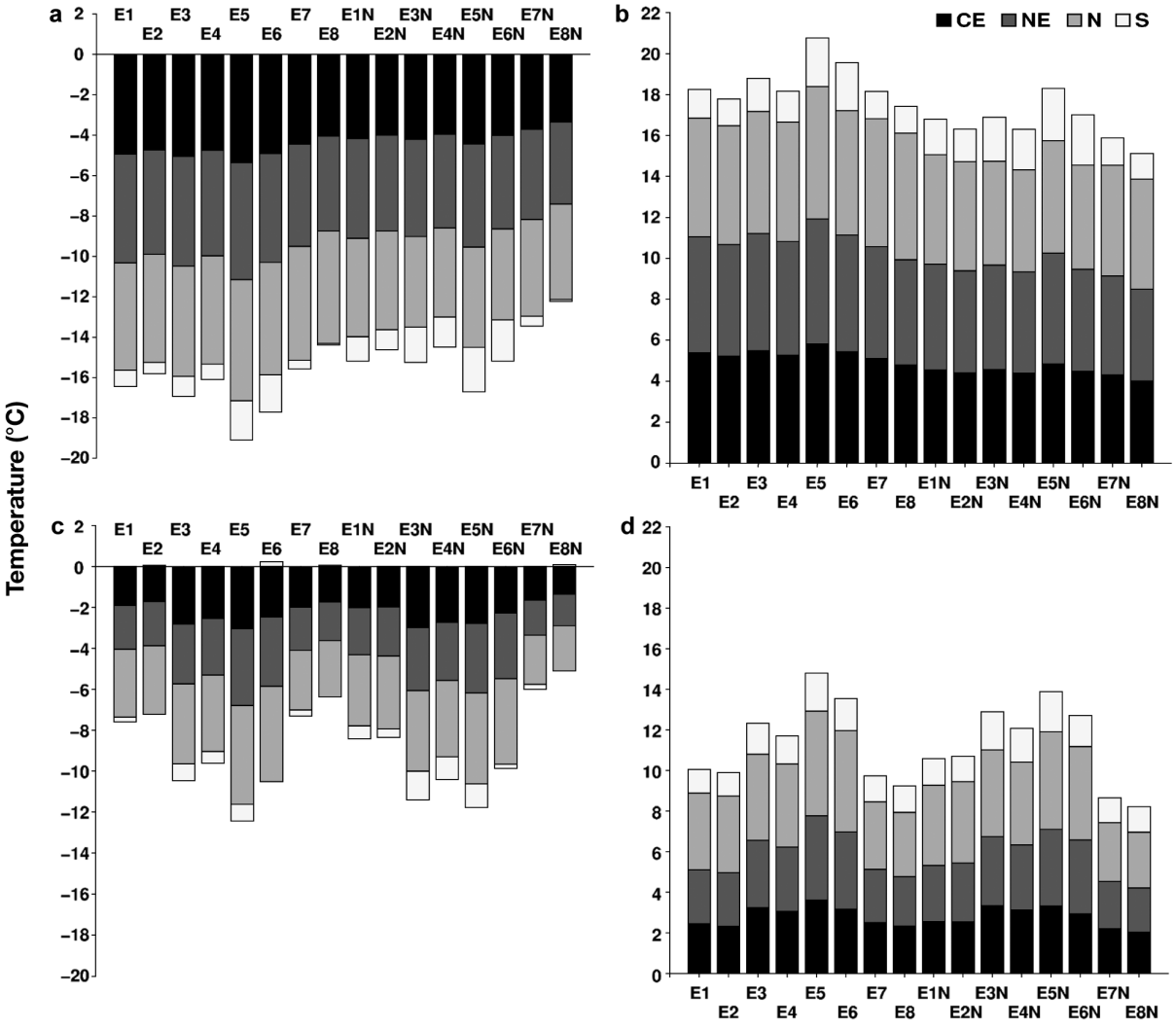


Fig. 2. Performance on temperature (°C) for (a,b) the dry season and (c,d) the wet season; (a,c) mean bias (MB), (b,d) RMSE. See Fig. 1 for definitions of sub-regions (CE, NE, N, S) and Table 1 for definitions of experiments (E1–E8 and E1N–E8N)

both seasons over most of Thailand, with the exception of the sub-regions N in the dry season and S in the wet season, and the degree of improvement (as compared to the other CPSs) was found to range from small (or negligible) to large, i.e. by 0.0 to 1.7°C for MB and 0.0 to 1.1°C for RMSE in the dry season, and by 0.0 to 2.0°C for MB and 0.0 to 1.9°C for RMSE in the wet season. Im et al. (2008) and Zanis et al. (2009) also used RegCM3, and obtained similar findings of temperature underestimation and bias reduction with EMU. Zanis et al. (2009) described the latter finding as a result of warmer near-surface temperature induced by EMU, which is attributed to stronger convection. This leads to more effective drying (i.e. condensation > evaporation) of the atmosphere, and then less moisture content and larger absorbed short-wave radiation at the surface. Considering the degree of contribution to model performance between CPS and OFS, the results from all experiments suggested that the former has a greater influence. The D1 experiments with the BATS scheme (E2, E4, E6, and E8) for OFS slightly improved or gave comparable results in terms of MB and RMSE for all sub-regions in both seasons, with the largest reductions of cold bias being 0.4°C in the dry season and 0.6°C in the wet season, in comparison to the Zeng scheme (E1, E3, E5, and E7). ERA40 near-surface air temperatures were generally higher than the simulated results (not shown), suggesting the systematic underestimation found in the present study to be potentially model-intrinsic (as opposed to effects from the reanalysis data used).

The nested finer-resolution (D2) simulations, similar to the D1 experiments, mostly produced poor results in both seasons and for all sub-regions, with the exception of sub-region S where MB ranged from −2.2°C to 0.1°C. Compared to the D1 results, the magnitudes of MB and RMSE in the dry season increased for S (by ≤0.7°C), but decreased for other sub-regions (by ≤1.1°C). A smaller degree of change was generally seen in the wet season for all sub-regions (≤0.6°C for MB magnitude and ≤0.4°C for RMSE). In the wet season, some nested simulations (E1N–E4N in which schemes AK and GAS were used) produced comparable or slightly worse results to those in D1 experiments for all sub-regions whereas the other simulations (E5N–E8N where schemes GFC and EMU were used), showed comparable or slightly better results. Nesting to D2 provided greater spatial detail (Fig. 3b,d). However, in terms of MB and RMSE, it did not necessarily improve performance for temperature, and its impact was not as large as the choice of CPS. Like the D1 experiments, the model showed a cold bias in both the dry and wet seasons, with the exception of sub-region S in simulation E8N.

In terms of daily variability (see Figs. S1 & S2 in the supplement at www.int-res.com/articles/suppl/c047 p171_supp.pdf), it depended on sub-region and season, and did not conclusively determine the optimal experiment(s). The dry season tended to have larger variability in both observed data and simulated results than the wet season, except for sub-region S. IQR ranged from 1.8 to 3.3°C (TMD) and from 1.3 to 4.5°C (simulated) in the upper sub-regions in the dry season and from 1.4 to 1.8°C (TMD) and from 0.8 to 2.7°C (simulated) in the wet season. The degree of variability was relatively small in sub-region S for both seasons in observed data (IQR = 1.2°C), which was also revealed by all experiments in the dry season, and by most experiments (6 out of 8 D1 or D2 experiments) in the wet season (IQR = 0.6 to 1.0°C). In the dry season, simulations using scheme EMU (E7 and E8, or E7N and E8N) gave larger variability (IQR = 2.8 to 4.5°C) than the other experiments for sub-regions CE and N while, in the wet season, larger variability was given by simulations using scheme GFC (E5 and E6, or E5N and E6N) for sub-regions CE and S (IQR = 1.6–2.7°C).

The spatial distributions of mean temperature biases relative to the gridded UDEL data are given in Figs. S3 & S4 in the supplement. All experiments show systematic underestimation in both seasons, with large cold biases (>2°C) for the upper sub-regions in the dry season and biases reduced by 1 to 2°C from the dry season to the wet season over Thailand. Schemes AK (experiments E1–E2 and E1N–E2N) and EMU (E7–E8 and E7N–E8N) gave higher temperatures than the other CPSs in the wet season over sub-regions NE and CE (thus closer predictions to observations). The D2 experiments with scheme EMU (E7–E8N) produced better results than those in the D1 experiments (E7–E8) for sub-regions NE and N in the wet season. These above findings are in accordance with those based on the TMD data. BATS tended to improve performance only in GAS (E4) and GFC (E6) experiments during the wet season over NE and S, in comparison with those using the Zeng scheme (E3 and E5), whereas with the data from the TMD, improvement by BATS could be also seen in AK (E2) and EMU (E8) for all sub-regions in both seasons.

### 3.2. Precipitation

Precipitation results are summarized in Fig. 4 (with more details given in Tables S3 & S4 in the supplement). In the observation data and all D1 experiments, discrepancies in precipitation amount between the 2 seasons over sub-regions CE, NE, and N were noticeable; e.g. (1) dry season, 0.4 to 0.9 mm $d^{-1}$ (mean values; TMD), and 0.1 to 2.6 mm $d^{-1}$ (simulated), and (2) wet season, 5.9 to 7.9 mm $d^{-1}$ (TMD) and 1.5 to 18.9 mm $d^{-1}$ (simulated) (Figs. S5 & S6 in the supplement). Sub-

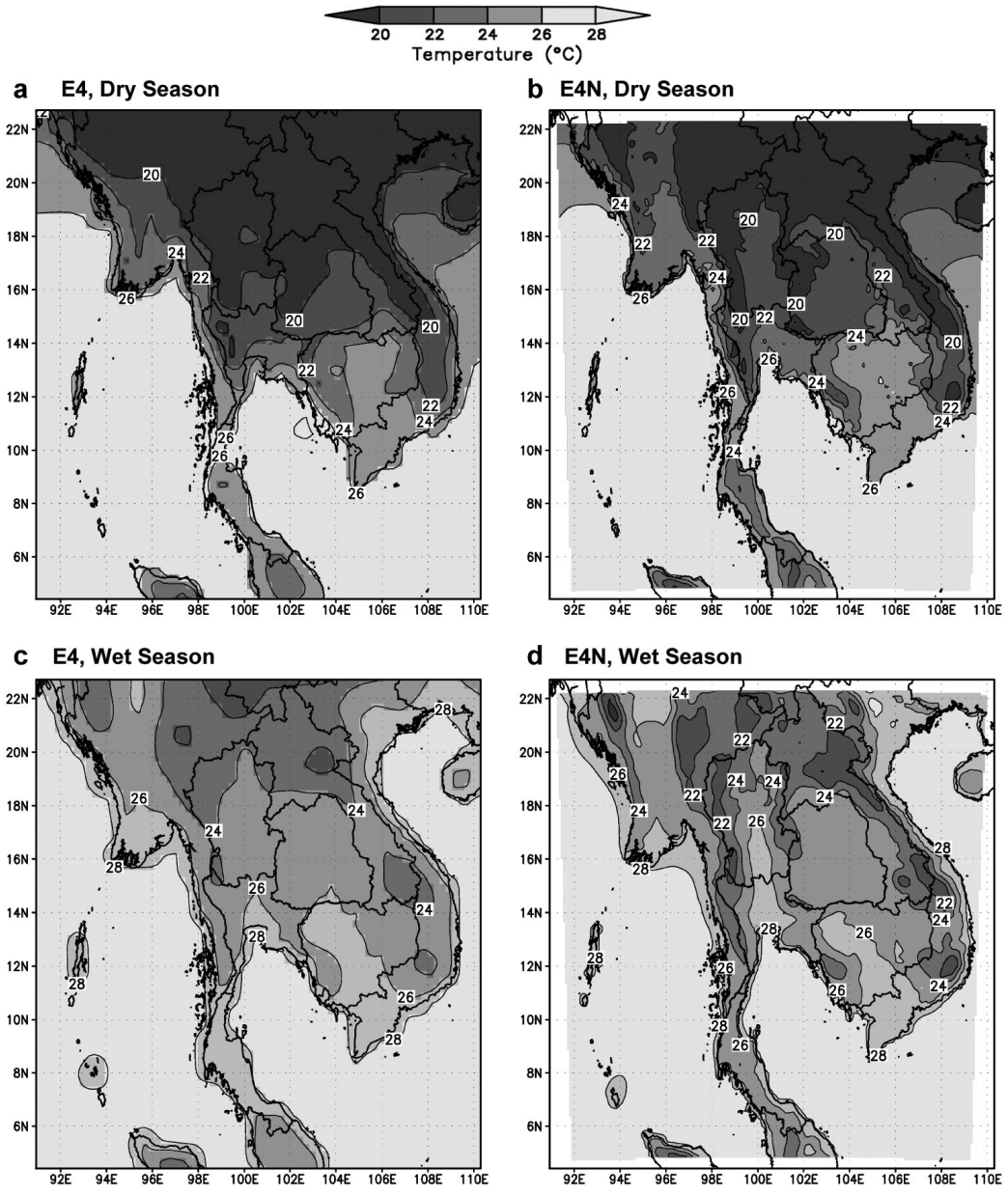


Fig. 3. Spatial distributions of simulated temperature in (a,b) the dry season and (c,d) the wet season for 2 selected experiments: (a,c) E4 (coarse resolution D1) and (b,d) E4N (finer resolution D2)

region S had a larger rainfall than the other sub-regions in the dry season, due to the geographical dependence of its climate (see Section 1), which was clearly shown by both observation data and the simulations. MB and RMSE magnitudes in the dry season were relatively small for sub-regions CE, NE, and N (MB = –0.5 to 1.8 mm $d^{-1}$, RMSE = 2.8 to 11.1 mm $d^{-1}$) and large for sub-region S (MB = –4.0 to 3.6 mm $d^{-1}$, RMSE = 19.2 to 30.8 mm $d^{-1}$). Nevertheless, normalized absolute MB (with respect to the observed mean) tended to be relatively low (<60%), while that in the other sub-regions ranged from 0 to 280%. In the wet season, both MB and RMSE increase (in terms of magnitude) for all sub-regions, with MB = –7.8 to 12.0 mm $d^{-1}$ and RMSE = 12.8 to 35.8 mm $d^{-1}$. In addition, the ranges of normalized absolute MB (with respect to the observed mean) were 3 to 200% for sub-regions CE, N, and NE, and 9 to 85% for S.

In both seasons, scheme AK (experiments E1 and E2) underestimated precipitation (i.e. dry biases) (largest MB = –7.8 mm $d^{-1}$). AK theoretically uses a closure based on moisture convergence, and convection itself is not directly caused by large-scale moisture supply, which is a critical drawback of the scheme (Raymond

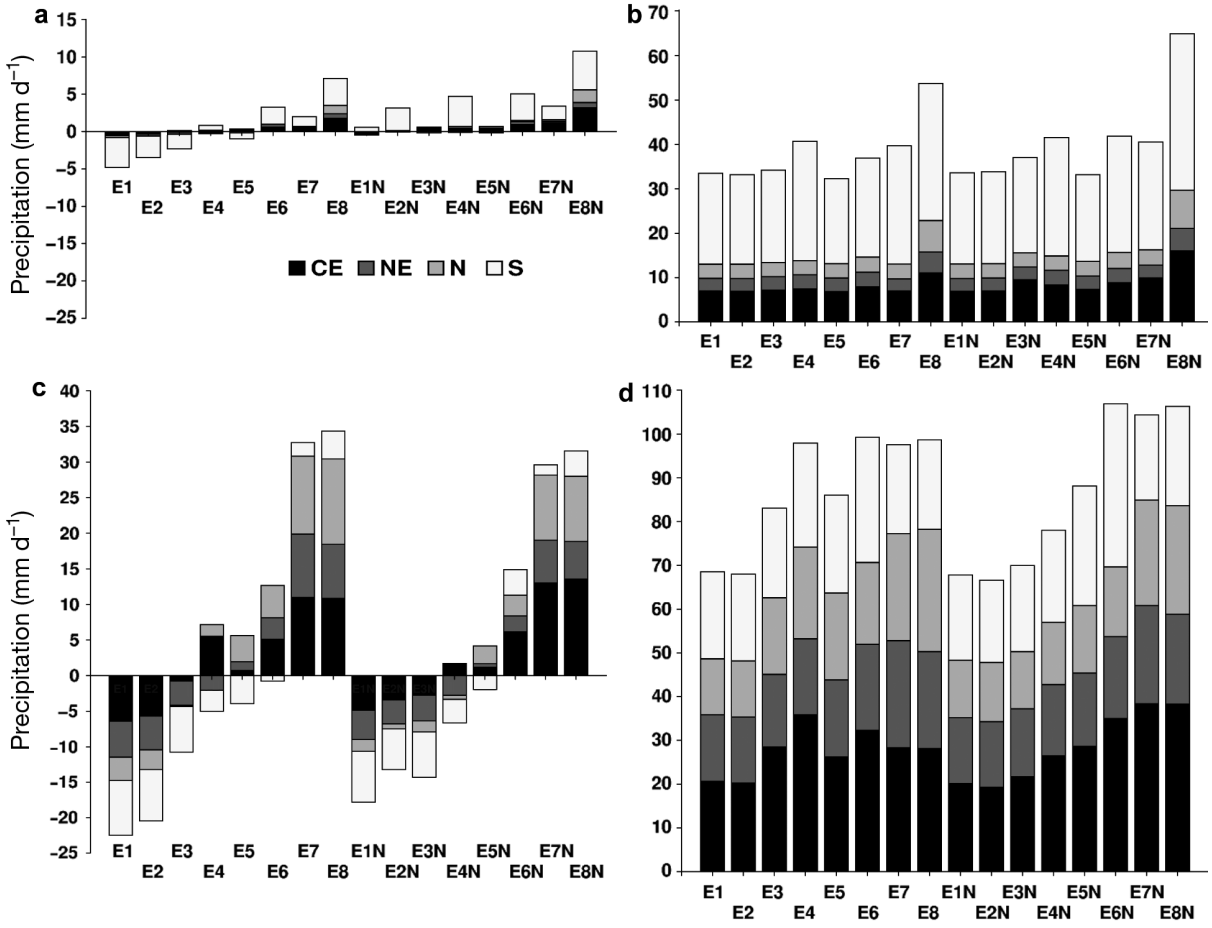


Fig. 4. Performance on precipitation for (a,b) the dry season and the (c,d) wet season: (a,c) MB, (b,d) RMSE

& Emanuel 1993). The results from schemes GAS (E3 and E4) and GFC (E5 and E6) were not conclusive, depending on OFS choice, season, and sub-region. Scheme EMU (E7 and E8) overestimated precipitation (i.e. wet biases), which were somewhat large in sub-regions CE, NE, and N during the wet season (MB = 7.6 to 12.0 mm d$^{-1}$). Such overestimation by EMU in the wet season over Thailand was also reported in Pal et al. (2007) where a RegCM3 simulation for South Asia (also including part of Southeast Asia) was performed. EMU gave more precipitation compared to GAS and GFC. Scheme EMU uses fewer requirements for convection to be triggered than Grell, resulting in more frequent triggering and a tendency to produce more precipitation (Im et al. 2008, Zanis et al. 2009). For the OFSs, BATS (experiments E2, E4, E6, and E8) yielded more precipitation than the Zeng scheme (E1, E3, E5, and E7) by 25 to 275% in the dry season and by 6 to 135% in the wet season, except for sub-regions CE and NE in experiments E4 (dry season) and E8 (wet season). Increased precipitation by BATS was also reported in the RegCM3 studies made by Francisco et al. (2006) and Martinez-Castro et al. (2006). Such increases are partially related to the overestimation of latent heat flux over ocean by BATS (Zeng et al. 1998), bringing more evaporation and moisture, and, when transported onshore, more precipitation over land. The overall performance given by BATS and the Zeng scheme was closely associated with the choice of CPS used. When both were combined with scheme AK (E1 and E2), the degree of difference in MB and RMSE was not large, but became pronounced with the other CPSs, i.e. precipitation by AK became least sensitive to the choice of OFS. With schemes GAS, GFC or EMU, which OFS is better was inconclusive in terms of MB, but in terms of RMSE, BATS gave a larger RMSE than the Zeng scheme in most results, with the largest difference in RMSE being 7.3 mm d$^{-1}$, as seen for region CE in E4 during the wet season (see Table S3b in the supplement).

Comparing the results from both domains (i.e. D2 experiments E1N–E8N and corresponding D1 experiments E1–E8), the nested finer-resolution (D2) modeling produced spatial patterns of precipitation

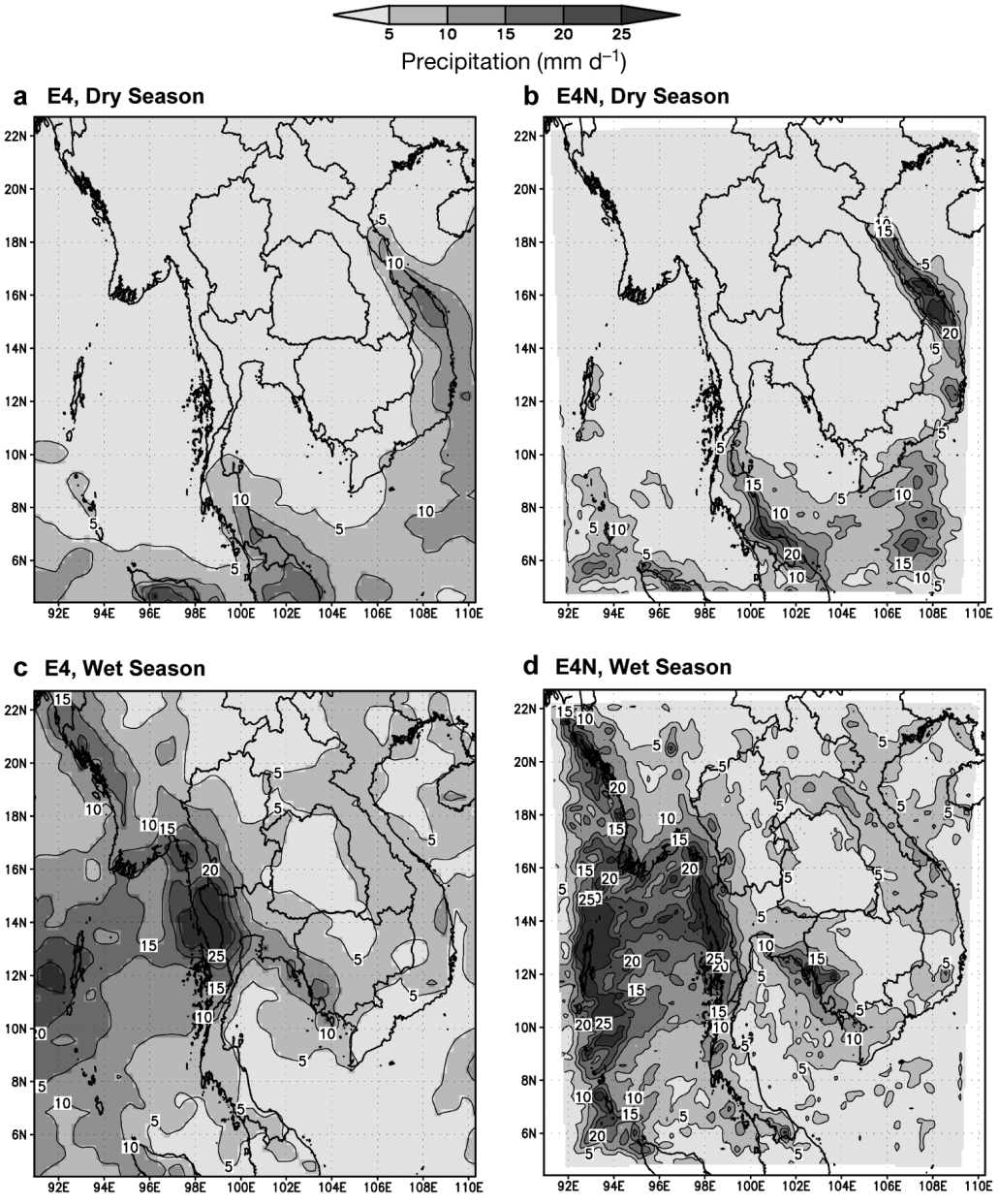


Fig. 5. Spatial distributions of simulated precipitation in (a,b) the dry season and (c,d) the wet season for 2 selected experiments: (a,c) E4, (b,d) E4N

similar (but enhanced) to those from the D1 experiments (Fig. 5). However, the overall performance may improve or deteriorate, and the effects of the D2 modeling were generally shown to be quite sensitive to CPS choice. When scheme AK was employed, the finer-resolution modeling tended to yield more precipitation in both seasons, which was mainly from a larger contribution of convective precipitation (not shown), and has MB differences (in terms of magnitude) between both domains being comparable or smaller (by <6 mm $d^{-1}$) and RMSE differences not varying much. This scheme tended to produce more precipitation at a finer resolution because its moisture convergence threshold can be reached more easily over a smaller grid cell. All D2 experiments showed increased precipitation for sub-region S during the dry season (by 0.5 to 5.9 mm $d^{-1}$), markedly (with a directional change from dry to wet biases) in those with scheme AK. In the wet season, the effects of the finer-resolution modeling on the overall precipitation performance varied. For instance, when scheme GAS was used, decreased precipitation was seen. Also, RMSE became smaller in every sub-region (by 0.8 to 9.4 mm $d^{-1}$). Schemes GFC and EMU showed mixed results in terms of precipita-

tion change direction and prediction performance improvement. The strongest influence due to the finer-resolution modeling with scheme GFC was in sub-region S during the wet season (where MB and RMSE changed by as much as 4.4 and 8.7 mm $d^{-1}$, respectively), and, with scheme EMU, was in sub-region CE during the wet season (where MB and RMSE change by as much as 2.7 and 10.2 mm $d^{-1}$, respectively). Similarly to the D1 experiments, BATS induced increased precipitation more than the Zeng scheme in all D2 experiments (except for sub-regions NE and N in experiment E8N). Note that EMU gave wet biases in the wet season across Thailand, and, when compared to GFC, gave more precipitation. Im et al. (2008), who conducted RegCM3 simulations over East Asia, reported similar findings for summer precipitation in the continental Korean Peninsula, and attributed the overestimation to increased convective precipitation induced by EMU. We also examined convective precipitation simulated by the D1 and D2 experiments associated with schemes GFC and EMU specifically and found that, using EMU, convective precipitation increased throughout Thailand (not shown).

For daily variability in precipitation, both observations and simulated results from all D1 and D2 experiments (Figs. S5 & S6 in the supplement) were in agreement in that the variability was typically small for sub-regions CE, NE and N in the dry season (IQR = 0 to 3.0 mm $d^{-1}$) and grew large for sub-region S in the dry season and for all sub-regions in the wet season, when IQR could be as large as 16.0 mm $d^{-1}$. It is seen that, for the dry season, experiments E7 and E7N (in which EMU and Zeng schemes were used) generally gave a fair (i.e. not too deviating) representation of the mean and variability of the observations for sub-region S. For the wet season, it may not be so readily seen that an experiment gave a good or adequate representation for most (or all) sub-regions. For example, in the D1 experiments, E5 could be a candidate configuration in sub-regions CE and NE but not in sub-regions N and S.

Comparison with the UDEL gridded data (Figs. S7 & S8 in the supplement) showed that the minimal or low precipitation observed over the upper sub-regions in the dry season was simulated in all experiments, except for experiment E8N which yielded wet bias (up to 10 mm $d^{-1}$ in the lowest part of sub-region CE). In the wet season, precipitation was not well simulated by most experiments, i.e. for most of Thailand, 6 (out of 16) (E1–E3 and E1N–E3N) showed dry bias while another 6 (E6–E8 and E6N–E8N) gave wet bias (>10 mm $d^{-1}$ over certain areas, as seen in E7–E8 and E7N–E8N). In the wet season, experiments E5 and E5N also tended to yield wet bias and gave the best performance over the CE and NE sub-regions. The above findings are fairly in line with those based on the TMD data. The nested finer-resolution (D2) modeling could help to improve the results (relative to the D1 results), especially over the upper sub-regions.

### 3.3. Synoptic winds

The average winds at 850 hPa from ERA40 and 3 selected experiments (E1, E4, and E7) are shown in Fig. 6. Those of the other experiments, together with those at 200 hPa, are given in Figs. S9 to S12 in the supplement. In the dry season, at 850 hPa, the ERA40 reanalysis data revealed easterlies over the Indian Ocean, westerlies over the Tibetan Plateau and northeasterlies over the South China Sea (Fig. 6, Fig. S9 in the supplement). Most experiments simulated the easterlies of the Indian Ocean (except experiment E6) but their spatial extents were extended to about 5 to 15°N latitude and their wind speeds were overestimated by ~5 m $s^{-1}$ (Fig. S9). The mid-latitude westerlies of the Tibetan Plateau were satisfactorily captured by every experiment while the northeasterlies over the South China Sea were shifted slightly westward, particularly in experiments E5 and E6. The choice between the 2 OFSs did not appear to have a great influence on simulated winds, except for experiments E5 and E6 (where scheme GFC is used) over the Indian Ocean. For the average 200 hPa winds in the dry season (Fig. S10 in the supplement), the equatorial easterlies from the reanalysis, moving southward to ~10° S and northward to ~10° N before turning eastward, were also simulated in every experiment. The mid-latitude westerly jet stream was also observed in both the reanalysis and all experiments.

In the wet season, the main features of the average 850 hPa winds in the ERA40 reanalysis data are (1) westerlies and southwesterlies in India and the Bay of Bengal, which then move across the Indochinese Peninsula and turn northward over the South China Sea and China (Fig. 6 & Fig. S11 in the supplement), (2) easterlies that prevail over 5 to 10° S latitude and show a northward shift in the lower-left portion of the domain (D1), and (3) the presence of cross-equatorial winds to the north. In general, these features were fairly reproduced by all experiments and better captured by E4 and E5. Using scheme AK (E1 and E2) yielded a large deviation from the reanalysis data over the Bay of Bengal (until near the equator) where winds moved toward the north and wind speed was underestimated, which could be a possible cause of the underestimation in precipitation over Thailand (by a range of MB from −7.8 to −2.8 mm $d^{-1}$) (see Table S3b in the supplement). Moreover, winds around the equator tended to show the opposite direction (compared to the reanalysis). However, overestimation in wind speed

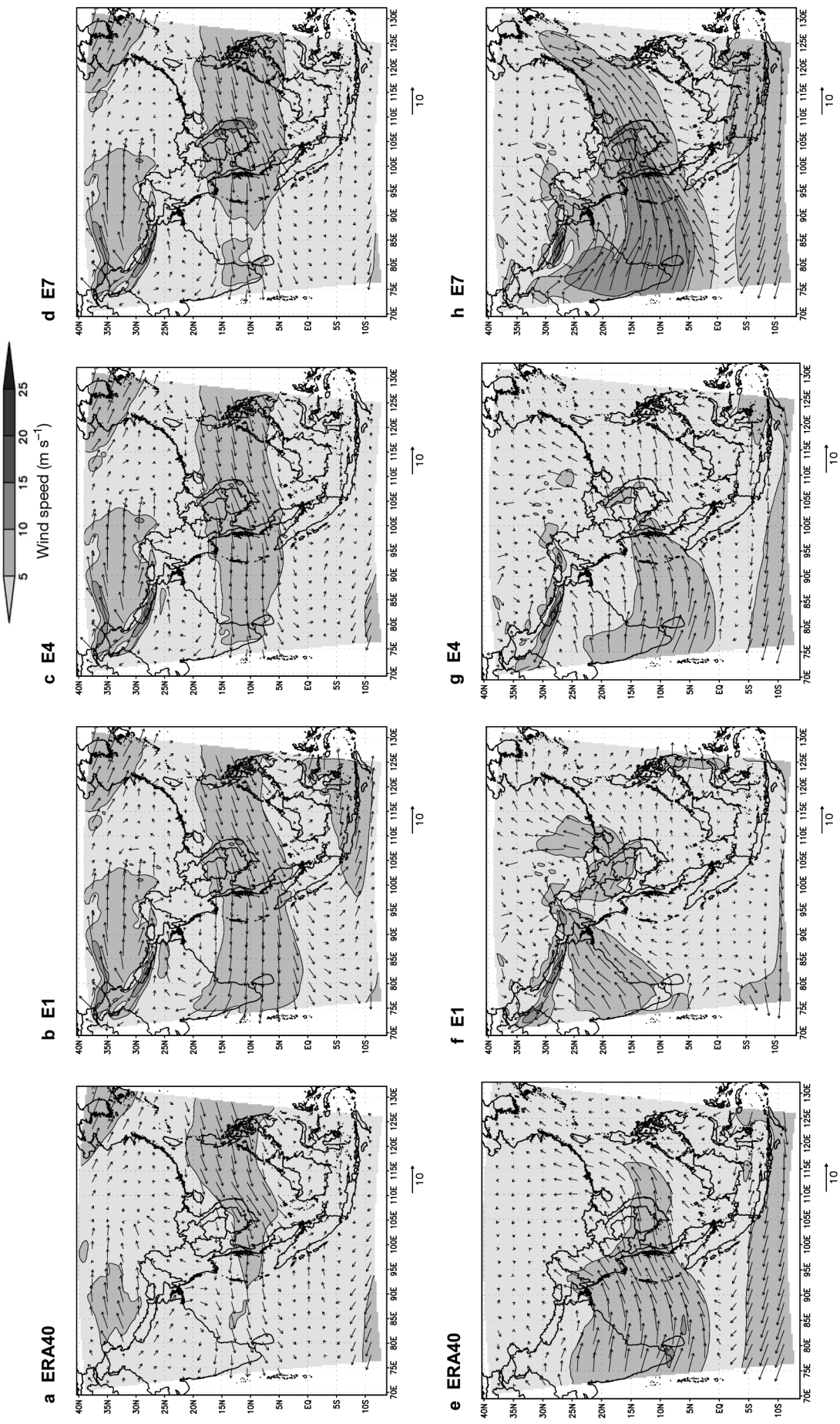


Fig. 6. Average winds at 850 hPa on D1 in (a–d) the dry season and (e–h) the wet season: (a,e) ERA40, (b–d), and (f–h) 3 selected experiments (E1, E4, and E7)

was found over the Bay of Bengal when using scheme EMU (E7 and E8), possibly leading to the positively biased results in precipitation for all of Thailand (MB = 1.9 to 12.0 mm $d^{-1}$). For the OFSs, BATS tended to yield slightly larger wind speed than Zeng et al. in many parts of the domain, e.g. from the Bay of Bengal to the South China Sea. For the average 200 hPa winds, an extended anticyclonic pattern over the Tibetan Plateau (Fig. S12 in the supplement) was consistently found in both the reanalysis data and all experiments. The northeasterlies in the South China Sea and the Indian Ocean, which were seen from the reanalysis data, were not as evident in experiments E1 to E3 as in the other experiments, and their magnitudes were overestimated in E5 to E8. The differences in synoptic winds among all D1 experiments were generally less noticeable than those in temperature and precipitation and also decreased with altitude (see 850 hPa and 200 hPa results in Fig. 6 and Figs S9-S10 in the supplement)). This can be attributed to the reduced influence of land-surface-related processes with altitude and the subsequent increased dependence on the lateral boundary conditions.

### 3.4. Land cover modification

From the findings obtained so far, the problem of temperature underestimation is serious for most parts of Thailand in both seasons (especially, the upper sub-regions during the dry season). The problem systematically existed across all 16 experiments, and they represented all possible combinations of the available CPSs and OFSs. Further investigation of this issue is needed. We examined one specific aspect, a land cover modification in the model. As seen in Fig. 7, the most dominant land cover type in Thailand (59% of the total land area) is 'irrigated crop', which is realistic due to agriculture being the largest economic sector, followed by 'evergreen broadleaf forest' (14%) and 'forest/field mosaic' (12%). From Kueppers et al. (2008), the BATS version 1e land-surface model used in RegCM3 prescribes very high soil moisture (i.e. at field capacity in all time steps) for 'irrigated crop' land cover, which tends to enhance latent heat flux and to reduce sensible heat flux, and then reduces near-surface air temperature. We hypothesized that this effect could play a substantial role in the large cold bias problem and examined it with an additional simulation test in which land cover was modified to another type as surrogate (here, 'crop/mixed farming'). We also rechecked the locations of the TMD stations used in the evaluation and found that most of them fall in grid cells of this land cover, especially those in the CE and NE sub-regions. The simulation was performed with the model setup in experiment E4 (using schemes GAS and BATS, and limited to the D1 domain) over the same periods as before. The choice of E4 did not imply or reflect a best model configuration, but rather a representative for testing. The results are shown in Table 2 (and also Fig. S13 in the supplement). Temperatures from the simulation using the modified land cover were higher than those using the default land cover during the dry season for the upper sub-regions (CE, NE, and N). When compared to the observed (TMD) data, the land cover modification improved performance substantially in the dry season (MB reduced by 2.2 to 3.3°C and RMSE by 1.8 to 2.8°C). No strong effect was seen in sub-region S, which is likely due to the minimal presence of 'irrigated crop' land cover in the sub-region and to the maritime climate conditions existing almost year round (resulting in relatively small seasonal soil moisture variations). In the wet season, no considerable change in temperature was found for all sub-regions

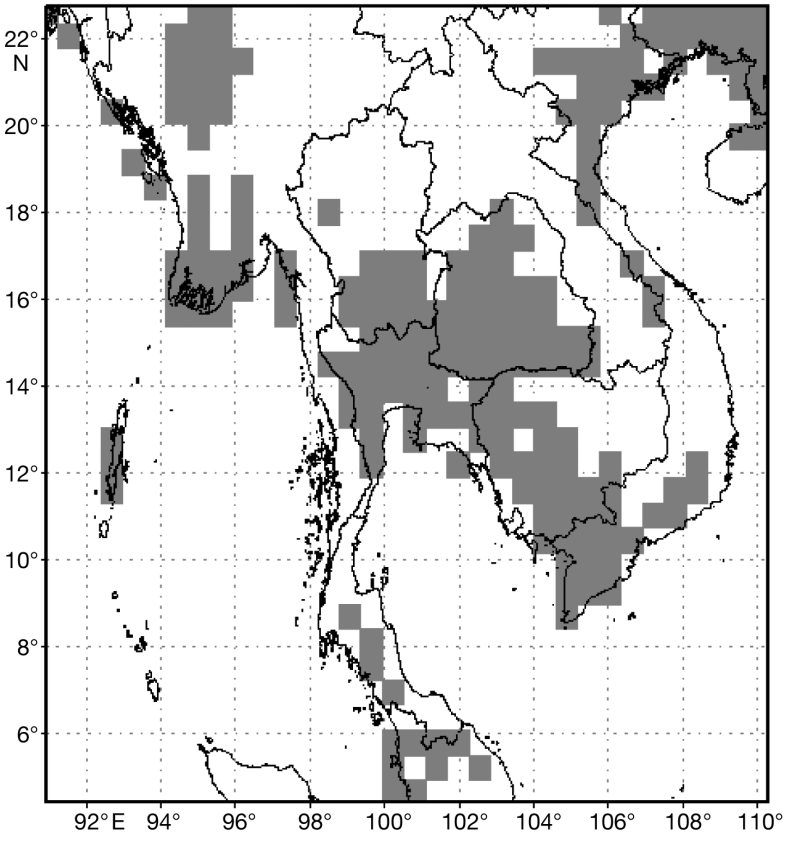


Fig. 7. Default areas (gray) designated as irrigated crop in D1. Note that only the central portion of D1 is shown above

Table 2. Performance on temperature (°C) and precipitation (mm $d^{-1}$) by sub-region in an additional simulation test using the modeling setup in E4 with default (Def.) and modified (Mod.; 'irrigated crop' to 'crop/mixed farming') land covers. MB: mean bias, RMSE: root mean square error

| Sub-region | Season | Temperature (°C) | | | | Precipitation (mm $d^{-1}$) | | | |
|---|---|---|---|---|---|---|---|---|---|
| | | MB | | RMSE | | MB | | RMSE | |
| | | Def. | Mod. | Def. | Mod. | Def. | Mod. | Def. | Mod. |
| Central-East (CE) | Dry | –4.7 | –1.7 | 5.3 | 2.5 | –0.1 | 0.0 | 7.5 | 7.7 |
| | Wet | –2.5 | –2.6 | 3.1 | 3.1 | 5.5 | 4.3 | 35.8 | 33.7 |
| Northeast (NE) | Dry | –5.2 | –1.9 | 5.5 | 2.7 | 0.2 | 0.2 | 3.2 | 3.7 |
| | Wet | –2.8 | –2.7 | 3.2 | 3.1 | –2.0 | –2.3 | 17.4 | 17.7 |
| North (N) | Dry | –5.4 | –3.2 | 5.8 | 4.0 | –0.2 | –0.1 | 3.2 | 3.5 |
| | Wet | –3.7 | –3.7 | 4.1 | 4.1 | 1.6 | 1.1 | 21.0 | 18.7 |
| South (S) | Dry | –0.8 | –0.8 | 1.5 | 1.6 | 0.7 | 0.2 | 26.9 | 26.8 |
| | Wet | –0.6 | –0.5 | 1.4 | 1.4 | –3.0 | –3.7 | 23.8 | 23.6 |

(–0.1 to 0.1°C), which is attributable to soil moisture difference being small or minimal between 'irrigated crop' and 'crop/mixed farming'. For precipitation, the performance using the modified land cover differed slightly (in terms of MB and RMSE) for all sub-regions in both seasons, when compared to the default land cover, but the differences may be relatively large in a few localities of each sub-region.

## 4. CONCLUSIONS

In this study, the prediction performance of regional climate model RegCM3 over Thailand and the effects of selected physical parameterizations and 1-way double nesting on (near-surface) temperature and precipitation were assessed, using a total of 16 numerical experiments formed by the available 4 convective and 2 ocean flux parameterization schemes, and conducted on coarse and fine resolution domains D1 (60 km) and D2 (20 km). The investigation also extended to the characteristics of upper-level synoptic winds. The simulations cover 8 dry and 8 wet season months in 1997–1999, and the model evaluation uses surface TMD data (primary) and the gridded UDEL data (supplementary) for temperature and precipitation, and the ERA40 reanalysis data for synoptic winds. An additional simulation was conducted to examine the change in model performance (with emphasis on temperature) due to a land cover modification (from 'irrigated crop' to 'crop/mixed farming'). A summary of key findings from the present study is given below.

(1) In both the coarse-resolution (D1) and nested finer-resolution (D2) experiments, systematic underestimation of temperature was found and was considerable for the upper sub-regions (i.e. CE, NE, and N) during the dry season (with the largest MB and RMSE being –6.0°C and 6.5°C, respectively). The substantial differences in precipitation between the dry and wet seasons, as observed for sub-regions CE, NE, and N, were reproduced by all experiments. The relatively high precipitation observed in the dry season over S (compared to the other sub-regions) were also well captured. The performance on temperature was generally better in the wet season compared to the dry season). For precipitation, no conclusion can be reached on the relative performances among the 16 main experiments, which were quite geographically and seasonally dependent.

(2) For convective parameterization, scheme EMU performed best, followed by AK, for temperature. However, in the wet season, EMU produced large overestimates for precipitation, particularly over sub-regions CE, NE, and N, whereas AK showed underestimates. Scheme GAS, when compared to GFC, yielded smaller cold biases, but the relative performances of these two schemes on precipitation were not clearly seen. For ocean flux parameterization, the BATS scheme, when compared to the Zeng scheme generally yielded better temperature results and tended to induce more precipitation.

(3) Although the nested finer-resolution (D2) modeling resulted in appreciably enhanced details spatially, it did not necessarily improve, and in some cases reduced, the quality of results over a particular sub-region. In the dry season, the D2 experiments increased MB and RMSE magnitudes for temperature in sub-region S (by ≤0.7°C) and generally showed more precipitation (compared to the corresponding D1 experiments using the same combination of physical parameterizations), while for the other sub-regions, a decrease in temperature (by ≤1.1°C) was seen. In the wet season, the differences in temperature between the D1 and D2 experiments were generally small (≤0.6°C) in all sub-regions, and no obvious conclusions could be reached on the effects of the finer-resolution modeling on overall precipitation performance, which varied with sub-regions and CPSs.

(4) The evaluation using the gridded UDEL data was helpful to compare the spatial patterns of the observed

and simulated quantities. Here, reasonable agreement was found with the evaluation using the TMD data on the following key findings: the presence of substantial cold bias over the upper sub-regions in the dry season and less cold bias in the wet season in all experiments; the relatively small bias in precipitation over these sub-regions in the dry season; and the tendency toward precipitation bias seen in the experiments during the wet season (e.g. dry bias over most parts of Thailand shown in experiments E1–E3 and E1N–E3N was found when using both datasets).

(5) All experiments reproduced fairly well the main seasonal features of synoptic winds, with better performance seen in the dry season. Scheme EMU produced overestimated wind speed at the 850 hPa level over the Bay of Bengal during the wet season, while AK produced underestimated wind speed over the same area. The BATS scheme induced slightly larger wind speed (at 850 hPa) than the Zeng scheme over the Bay of Bengal and the South China Sea in the wet season.

(6) It is evident that none of the experiments (using the default inputs and options in the model) yielded results that were satisfactory over all of Thailand, and that model performance was geographically and seasonally dependent. The most serious problem found is the systematic underestimation of temperature, suggesting further investigation on the representations of physical processes in the model or on potential model customization, is needed. In our additional simulation test with a land cover modification (converting 'irrigated crop', as the most dominant default land cover in Thailand, to 'crop/mixed farming', as a surrogate), the magnitude of the cold bias was lowered, markedly, in the dry season for the upper sub-regions (MB reduced by 2.2 to 3.3°C and RMSE by 1.8 to 2.8°C). This technique seems promising and potentially useful for future applications over this sub-region, but the test is still considered preliminary and limited.

Although this study aimed to understand the capability, strengths and weaknesses of RegCM3 for its application to Thailand, the assessment conducted in the present study is not comprehensive, and the findings are limited to the current spatial coverage. The model performance issue presented here should be examined in depth in future studies, e.g. land cover treatment of the current land surface model, use or development of a new or alternative land surface model and its coupling with RegCM3, and model customization by tuning or optimizing some parameters in a particular physical parameterization scheme. Moreover, the temporal coverage for the current study is relatively short-term (i.e. limited to 3 yr), and extending simulations for a longer period could be essential for the support of studies on e.g. long-term climate variability, climate change, and climate extremes.

*Acknowledgements.* This study was financially supported by the Joint Graduate School of Energy and Environment (JGSEE) and by the Thailand Research Fund under Grant Nos. RDG5050016 and RDG5030034. The authors sincerely thank the Abdus Salam International Center for Theoretical Physics for the availability of RegCM3 and its technical support, the European Centre for Medium-Range Weather Forecasts for the ERA40 reanalysis data, the Thai Meteorological Department for the observed data, and the University of Delaware for the gridded climatic data. The authors also appreciate several technical helpful comments and suggestions from Dr. Gao Xuejie (Chinese Meteorological Administration) and the kind encouragement from Dr. Sirintornthep Towprayoon (JGSEE) and Dr. Robert H. B. Exell (JGSEE), given along the course of the implementation of this study. Special thanks go to the people at the JGSEE Computational Laboratory (Bang Khun Tien Campus) for their general assistance. Lastly, we sincerely thank anonymous reviewers for their comments which improved our manuscript, particularly the suggestion of a land cover modification in the modeling.

## LITERATURE CITED

Anthes RA (1977) A cumulus parameterization scheme utilizing a one-dimensional cloud model. Mon Weather Rev 105:270–286

Arakawa A, Schubert WH (1974) Interaction of a cumulus cloud ensemble with the large-scale environment, part 1. J Atmos Sci 31:674–701

Christensen JH, Hewitson B, Busuioc A, Chen A and others (2007) Regional climate projections. In: Solomon S, Qin D, Manning M, Chen Z and others (eds) Climate change 2007: the physical science basis. Contribution of Working Group I to the Fourth Assessment Report of the Intergovernmental Panel on Climate Change. Cambridge University Press, Cambridge

Dickinson RE, Henderson-Sellers A, Kennedy PJ (1993) Biosphere Atmosphere Transfer Scheme (BATS) version 1e as coupled to the NCAR community climate model. NCAR Technical Note NCAR/TN-387+STR, 72

Elguindi N, Bi X, Giorgi F, Nagarajan B and others (2006) RegCM version 3.1: user's guide. http://users.ictp.it/RegCNET (accessed 27 Dec 2006)

Emanuel KA (1991) A scheme for representing cumulus convection in large-scale models. J Atmos Sci 48:2313–2335

Emanuel KA, Zivkovic-Rothman M (1999) Development and evaluation of a convection scheme for use in climate models. J Atmos Sci 56:1766–1782

Francisco RV, Argete J, Giorgi F, Pal JS, Bi X, Gutowski WJ (2006) Regional model simulation of summer rainfall over the Philippines: effect of choice of driving fields and ocean flux schemes. Theor Appl Climatol 86:215–227

Fritsch JM, Chappell CF (1980) Numerical prediction of convectively driven mesoscale pressure systems. I. Convective parameterization. J Atmos Sci 37:1722–1733

Gao X, Xu Y, Zhao Z, Pal JS, Giorgi F (2006) On the role of resolution and topography in the simulation of East Asia precipitation. Theor Appl Climatol 86:173–185

Giorgi F, Marinucci MR, Bates GT (1993a) Development of a second-generation regional climate model (RegCM2). I. Boundary layer and radiative transfer processes. Mon Weather Rev 121:2794–2813

Giorgi F, Marinucci MR, Bates GT, de Canio G (1993b) Development of a second-generation regional climate model (RegCM2). Part II. Convective processes and assimilation of lateral boundary conditions. Mon Weather Rev 121: 2814–2832

Giorgi F, Hewitson B, Christensen JH, Hulme M and others (2001) Regional climate information-evaluation and projections. In: Houghton JT, Ding Y, Griggs DJ, Noguer M, van der Linden PJ, Xiaoxu D (eds) Climate change 2001: the scientific basis. Contribution of Working Group I to the Third Assessment Report of the Intergovernmental Panel on Climate Change. Cambridge University Press, Cambridge, p 583–638

Grell GA (1993) Prognostic evaluation of assumptions used by cumulus parameterizations. Mon Weather Rev 121: 764–787

Grell GA, Dudhia J, Stauffer DR (1994) A description of the fifth-generation Penn State/NCAR Mesoscale Model (MM5). NCAR Technical Note NCAR/TN-398+IA, 121

Holtslag AAM, de-Bruijn EIR, Pan HL (1990) A high resolution air mass transformation model for short-range weather forecasting. Mon Weather Rev 118:1561–1575

Im ES, Ahn JB, Remedio AR, Kwon WT (2008) Sensitivity of the regional climate of East/Southeast Asia to convective parameterizations in the RegCM3 modeling system. I. Focus on the Korean Peninsula. Int J Climatol 28:1861–1877

Kiehl JT, Hack JJ, Bonan GB, Boville BA, Breigleb BP, Williamson DL, Rasch PJ (1996) Description of the NCAR Community Climate Model (CCM3). NCAR Technical Note NCAR/TN-420+STR, 152

Kueppers ML, Snyder MA, Sloan LC, Cayan D and others (2008) Seasonal temperature responses to land-use change in the western United States. Global Planet Change 60: 250–264

Loveland TR, Reed B, Ohlen DO, Zhu J, Yang L, Merchant J (2000) Development of a global land cover characteristics database and IGBP DISCover from 1-km AVHRR data. Int J Remote Sens 21:1303–1330

Martinez-Castro D, da-Rocha RP, Bezanilla-Morlot A, Alvarez-Escudero L, Reyes-Fernandez JP, Silva-Vidal Y, Arritt RW (2006) Sensitivity studies of the RegCM3 simulation of summer precipitation, temperature and local wind field in the Caribbean region. Theor Appl Climatol 86: 5–22

Matsuura K, Willmott CJ (2009a) Terrestrial air temperature: 1900–2008 gridded monthly time series (Version 2.01), Center for Climatic Research, Department of Geography, University of Delaware, http://climate.geog.udel.edu/~climate/html_pages/Global2_Ts_2009/README.global_t_ts_2009.html (accessed December 2010)

Matsuura K, Willmott CJ (2009b) Terrestrial precipitation: 1900–2008 gridded monthly time series, Version 2.01, Center for Climatic Research, Department of Geography, University of Delaware, http://climate.geog.udel.edu/~climate/html_pages/Global2_Ts_2009/README.global_p_ts_2009.html (accessed December 2010)

Pal JS, Small EE, Eltahir EAB (2000) Simulation of regional-scale water and energy budgets: representation of subgrid cloud and precipitation processes within RegCM. J Geophys Res 105:29579–29594

Pal JS, Giorgi F, Bi X, Elguindi N and others (2007) Regional climate modeling for the developing world: the ICTP RegCM3 and RegCNET. Bull Am Meteorol Soc 88:1395–1409

Phan VT, Ngo-Duc T, Ho TMH (2009) Seasonal and interannual variations of surface climate elements over Vietnam. Clim Res 40:49–60

Raymond DJ, Emanuel KA (1993). The Kuo cumulus parameterization. In: Emanuel KA, Raymond DJ (eds) The representation of cumulus convection in numerical models of the atmosphere. Meteorol Monogr Am Meteorol Soc 46: 145–147

Reynolds RW, Rayner NA, Smith TM, Stokes DC, Wang W (2002) An improved *in situ* and satellite SST analysis for climate. J Clim 15:1609–1625

Seth A, Giorgi F (1998) The effects of domain choice on summer precipitation simulation and sensitivity in a regional climate model. J Clim 11:2698–2714

Southeast Asia START Regional Center (2009) Future climate projection for Thailand and mainland southeast Asia using PRECIS and ECHAM4 climate models. In: Chinvanno S, Laung-Aram V, Sangmanee C (eds) Southeast Asia START Regional Center Technical Report No 18. http://www.start.or.th/documents/technical-reports/START%20Technical%20report%20no%2018%20-%20CC%20scenarios_v3.pdf/view (accessed 08 Feb 2010)

TMD (Thai Meteorological Department) (2008) Climate of Thailand. www.tmd.go.th (accessed 18 Nov 2008)

Uppala SM, Kållberg PW, Simmons AJ, Andrae U and others (2005) The ERA-40 re-analysis. Q J R Meteorol Soc 131: 2961–3012

USGS (United States Geological Survey) (1996) Global 30-arc-second elevation data (GTOPO30). http://eros.usgs.gov/Find_Data/Products_and_Data_Available/gtopo30_info (accessed Feb 2010)

Zanis P, Douvis C, Kapsomenakis I, Kioutsioukis I, Melas D, Pal JS (2009) A sensitivity study of the Regional Climate Model (RegCM3) to the convective scheme with emphasis in central eastern and southeastern Europe. Theor Appl Climatol 97:327–337

Zeng X, Zhao M, Dickinson RE (1998) Intercomparison of bulk aerodynamic algorithms for the computation of sea surface fluxes using TOGA-COARE and TAO data. J Clim 11:2628–2644

*Editorial responsibility: Filippo Giorgi, Trieste, Italy*

*Submitted: May 27, 2010; Accepted: January 14, 2011*
*Proofs received from author(s): May 14, 2011*